

## Electronic Supplementary Information

# Tetraphenylethylene-DNA Conjugates: Influence of Sticky Ends and DNA Sequence Length on the Supramolecular Assembly of AIE-Active Vesicles

Simon Rothenbühler,<sup>a</sup> Adrian Gonzalez,<sup>a</sup> Ioan Iacovache,<sup>b</sup> Simon M. Langenegger,<sup>a</sup>  
Benoît Zuber<sup>b</sup> and Robert Häner<sup>a\*</sup>

<sup>a</sup> Department of Chemistry, Biochemistry and Pharmaceutical Sciences, University of Bern,  
Freiestrasse 3, CH – 3012 Bern, Switzerland

<sup>b</sup> Institute of Anatomy, University of Bern, Baltzerstrasse 2, CH – 3012 Bern, Switzerland

## Table of contents

1. General methods .....	S1
2. Solid-phase oligomer synthesis .....	S2
3. UV-Vis and fluorescence spectra .....	S9
4. AFM images .....	S13
5. DLS.....	S18
6. Cryo-EM images.....	S18
7. Bibliography .....	S19

### 1. General methods

All reagents and solvents were purchased from commercial suppliers and used without further purification. The synthesis of (*E*)-4-(4-(2-(4-(4-(bis(4-methoxyphenyl)(phenyl)methoxy)but-1-yn-1-yl)phenyl)-1,2-diphenylvinyl) phenyl)but-3-yn-1-yl (2-cyanoethyl) diisopropylphosphoramidite, required for the solid-phase synthesis of the tetraphenylethylene (TPE)-modified oligonucleotides, followed published procedures.<sup>1</sup> Unmodified DNA single strands were purchased from Microsynth (Switzerland). Water was used from a Milli-Q system. Mass spectra were obtained from the Analytical Research and Services (ARS) of the University of Bern, Switzerland, on a Thermo Fisher LTQ Orbitrap XL using Nano Electrospray Ionization (NSI). All mass spectra were measured in negative ion mode in mixtures of acetonitrile/water/triethylamine. UV-Vis spectra were recorded on an Agilent Cary 100 spectrophotometer using quartz cuvettes with an optical path of 1 cm. Fluorescence spectra were collected on a Cary Eclipse fluorescence spectrophotometer using an excitation slit of 2.5 nm and an emission slit of 5 nm. Spectroscopic data were measured from at least five minutes thermally equilibrated samples at the corresponding temperature. Supramolecular assembly proceeded *via* thermal disassembly and reassembly: the sample solution was heated to 75 °C, followed by a controlled cooling of 0.5 °C/min to 20 °C in a Cary Eclipse fluorescence spectrophotometer equipped with a Peltier thermostat. Atomic force microscopy (AFM) experiments were conducted on a Nanosurf FlexAFM instrument in tapping mode under ambient conditions. AFM samples were prepared on (3-aminopropyl)triethoxysilane (APTES)-modified mica sheets (Glimmer “V1”, 20 mm x 20 mm, G250-7, Plano GmbH) according to published procedures, using a sample adsorption time of 7 min.<sup>1</sup> Dynamic light scattering (DLS) experiments were performed on a Malvern Zetasizer Nano Series instrument ( $\lambda = 633$  nm) in particle size distribution (PSD) mode (number value) at 25 °C. Samples for cryo-EM were plunge frozen using the FEI Vitrobot Mark 4 at room temperature and 100% humidity.

In brief, copper lacey carbon grids were glow discharged (air – 10 mA for 20 seconds). 3  $\mu\text{L}$  of the sample were pipetted on the grids and blotted for 3 seconds before plunging into liquid ethane. Sample grids were stored in liquid nitrogen. Images were acquired using a Gatan 626 cryo holder on a Falcon III equipped FEI Tecnai F20 in nanoprobe mode. Due to the nature of the sample, acquisition settings had to be adjusted for a low total electron dose (less than  $20 \text{ e}^-/\text{\AA}^2$ ) using EPU software. Distance measurements were done in Fiji<sup>2,3</sup> using the multi-point tool to set marks. After the read-out of the x- and y-values, the distances between the marks were calculated. The reported distances are mean values with the corresponding standard deviation.

## 2. Solid-phase oligomer synthesis

All TPE-DNA conjugates **ON1-ON5** (Table S1) were synthesized on an Applied Biosystems 394 DNA/RNA synthesizer applying a standard cyanoethyl phosphoramidite coupling protocol on a 1  $\mu\text{mol}$  scale. A coupling time of 30 s was employed for the DNA nucleobases (0.1 M in anhydrous acetonitrile) and 2 min for TPE phosphoramidite (0.1 M solution in anhydrous 1,2-dichloroethane). The synthesis was started with an TPE-modified long chain alkylamine controlled pore glass (LCAA-CPG) solid-support, which was prepared according to previously reported procedures.<sup>1</sup> After the solid-phase synthesis, **ON1-ON5** were cleaved and deprotected by treatment with aqueous  $\text{NH}_4\text{OH}$  (28-30%) at 55 °C overnight. The supernatants were collected, and the solid-support was washed three times with a solution of ethanol and Milli-Q  $\text{H}_2\text{O}$  (1:1, 3x1 mL), before the crude TPE-DNA conjugates were lyophilized.

All TPE-DNA conjugates **ON1-ON5** were purified by reversed-phase HPLC (*Shimadzu LC-20AT, LiChrospher 100 RP-18*, 5  $\mu\text{m}$ , 250 x 4 mm) at 50 °C with a flow rate of 1 mL/min,  $\lambda$ : 330 nm. Solvent A: aqueous 2.1 mM triethylamine (TEA) / 25 mM 1,1,1,3,3,3-hexafluoropropan-2-ol (HFIP) pH 8; solvent B: acetonitrile; applying the gradients listed in Table S1. The purified TPE-DNA conjugates **ON1** and **ON2** were dissolved in Milli-Q  $\text{H}_2\text{O}$  (1 mL), **ON3-ON5** were dissolved in a 1:1 ethanol/Milli-Q  $\text{H}_2\text{O}$  mixture (1 mL). The absorbance was measured at 260 nm to determine the concentration of the stock solutions and the yields of **ON1-ON5**. The calculation was according to the Beer-Lambert law. The following molar absorptivities (at 260 nm) in [L/mol·cm] were used for the DNA nucleobases:  $\epsilon_{\text{A}}$ : 15'300;  $\epsilon_{\text{T}}$ : 9'000;  $\epsilon_{\text{G}}$ : 11'700;  $\epsilon_{\text{C}}$ : 7'400. A molar absorptivity of  $\epsilon_{\text{TPE}}$ : 35'975 was used for TPE. The corresponding HPLC traces and mass spectra of **ON1-ON5** are displayed in Fig. S1 and Fig. S2–Fig. S6, respectively.

**Table S1** TPE-DNA oligonucleotide sequences **ON1-ON5**, HPLC gradients, calculated and found masses by NSI-MS, and yields.

Oligomer	Sequence (5'→3')	HPLC gradient B [%] ( $t_R$ [min])	calc. mass	found mass	Yield [%]
<b>ON1</b>	(TPE)-CTT CCT TGC ATC GGA CCT TG-(TPE)	5 (0), 40 (24)	7095.2951	7095.3432	10
<b>ON2</b>	(TPE) <sub>2</sub> -CTT CCT TGC ATC GGA CCT TG-(TPE) <sub>2</sub>	5 (0), 40 (24)	8155.6448	8155.6722	9
<b>ON3</b>	(TPE) <sub>3</sub> -CTT CCT TGC ATC GGA CCT TG-(TPE) <sub>3</sub>	5 (0), 50 (24)	9215.9945	9216.0492	25
<b>ON4</b>	(TPE) <sub>3</sub> -CTT CCT TGG ACC TTG-(TPE) <sub>3</sub>	5 (0), 50 (24)	7691.0132	7690.7916	21
<b>ON5</b>	(TPE) <sub>3</sub> -CTT CCT TGC ACT GAA TCG GAC CTT G-(TPE) <sub>3</sub>	5 (0), 50 (24)	10765.0008	10765.2660	7

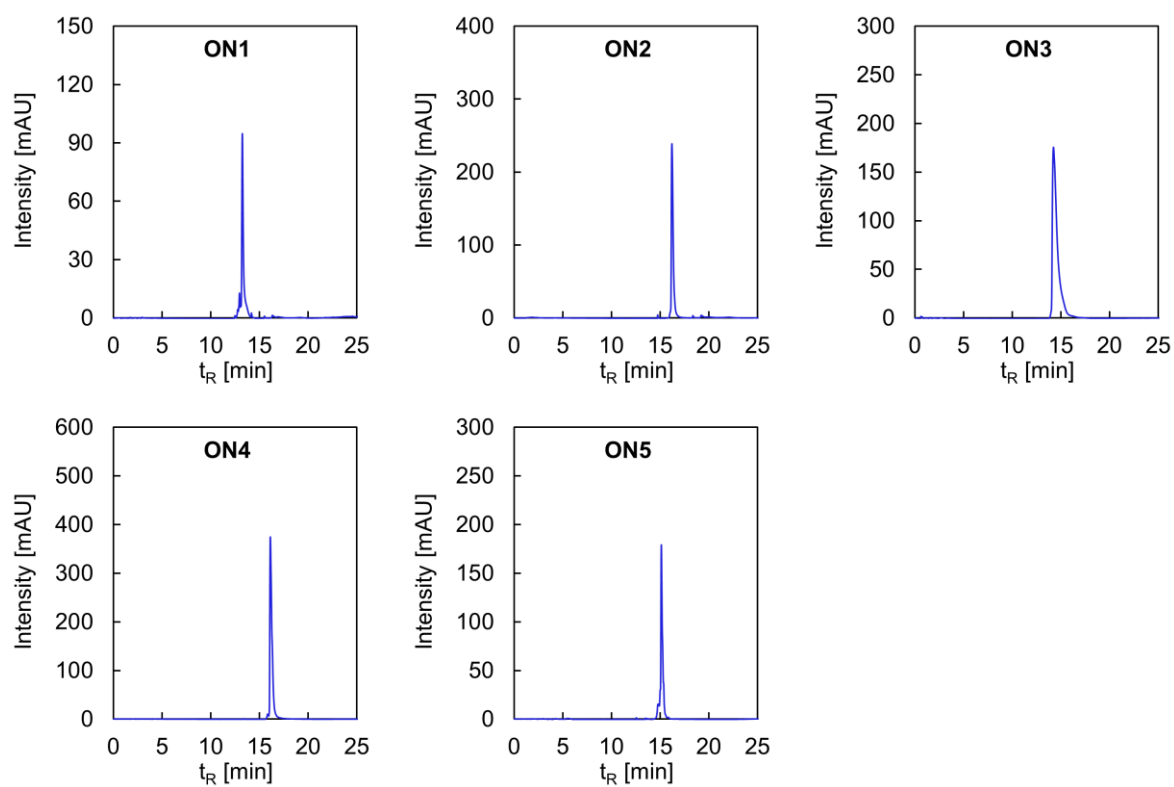


**Fig. S1** HPLC traces of **ON1-ON5**.

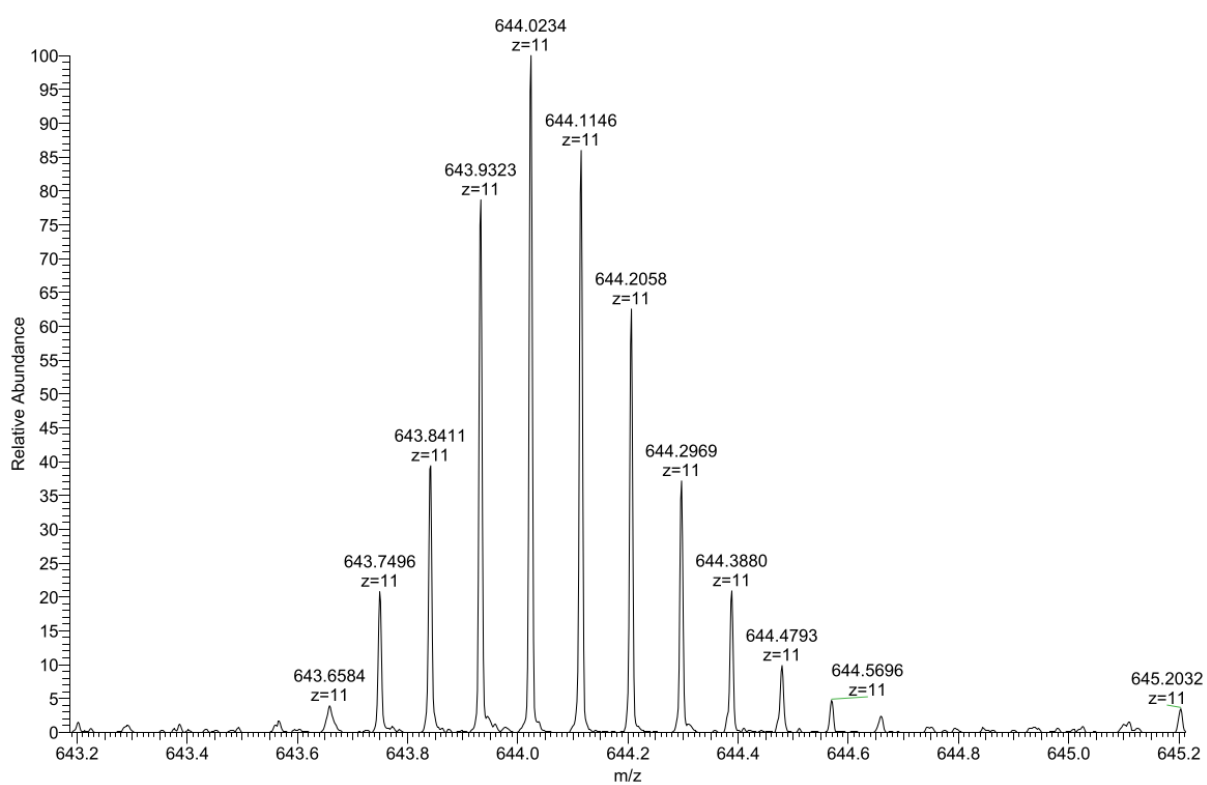
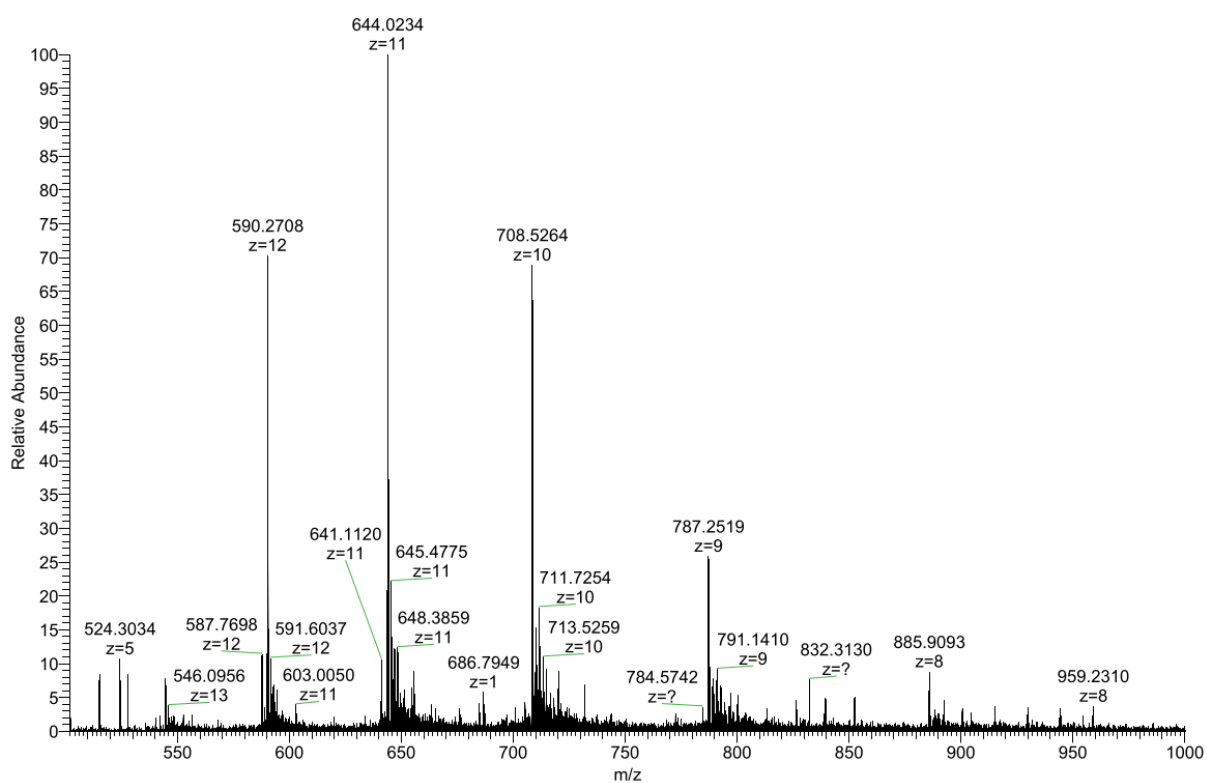


Fig. S2 MS spectra of ON1.

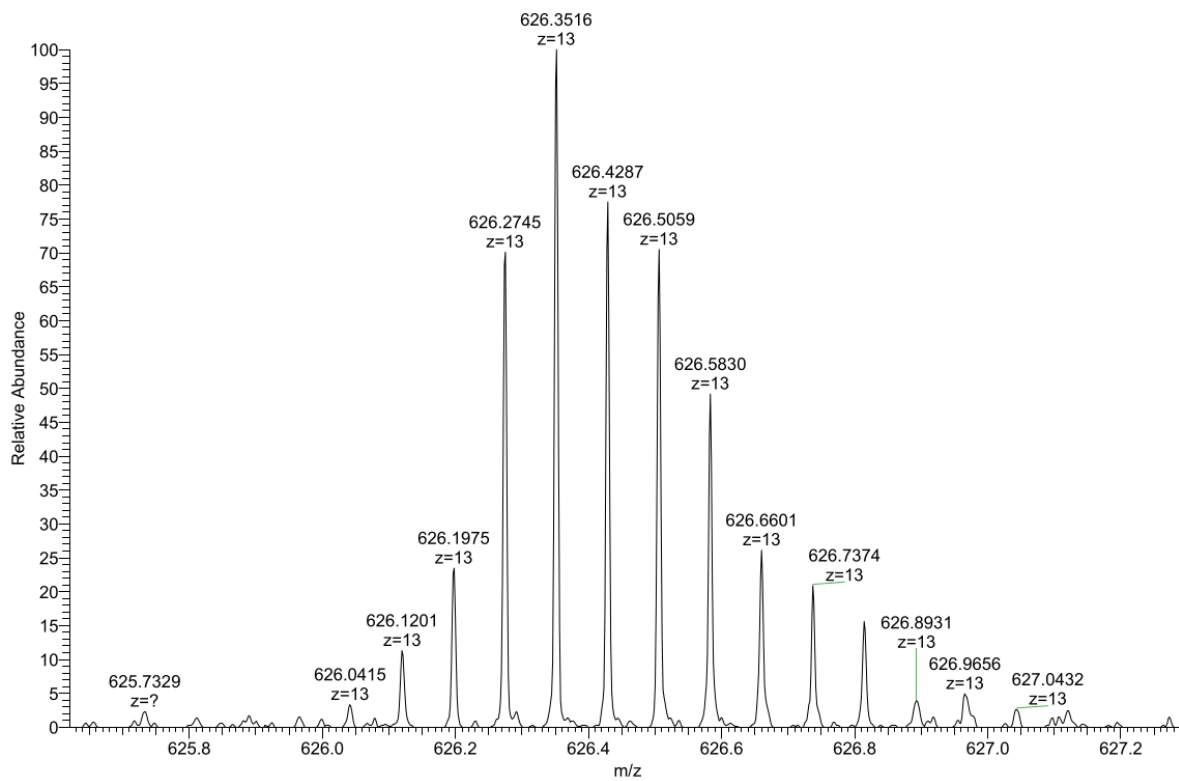
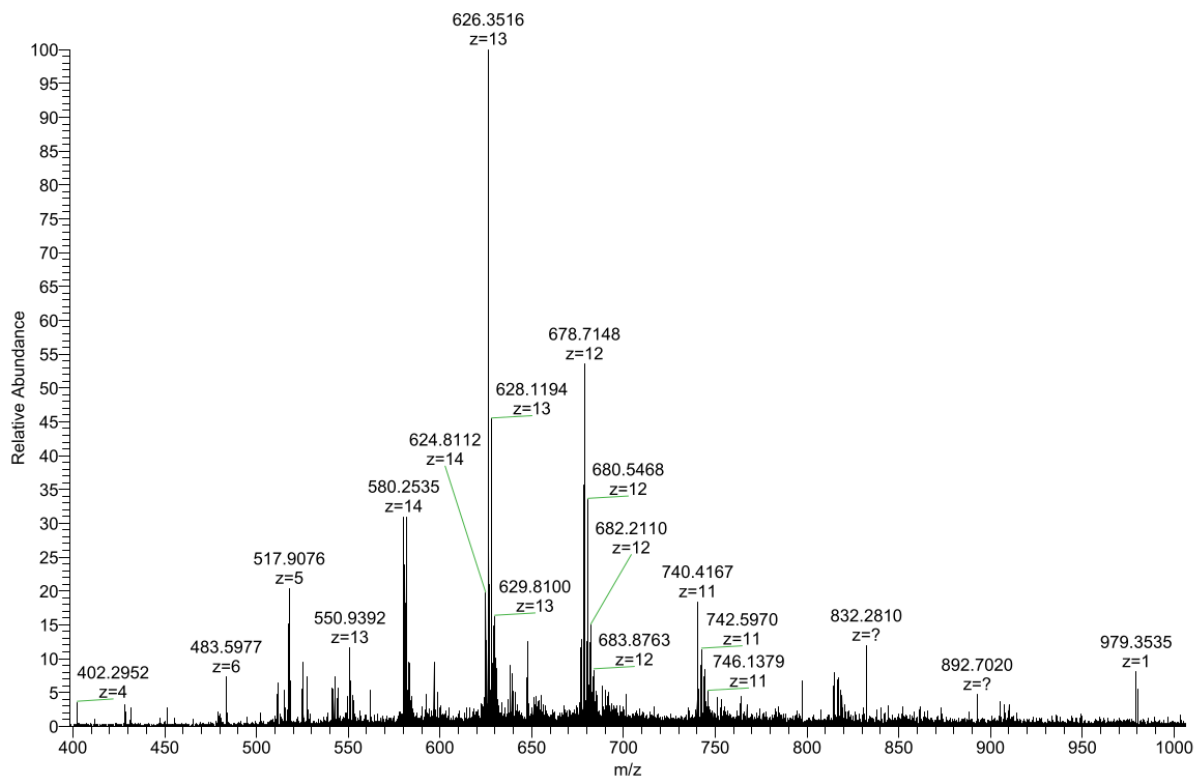
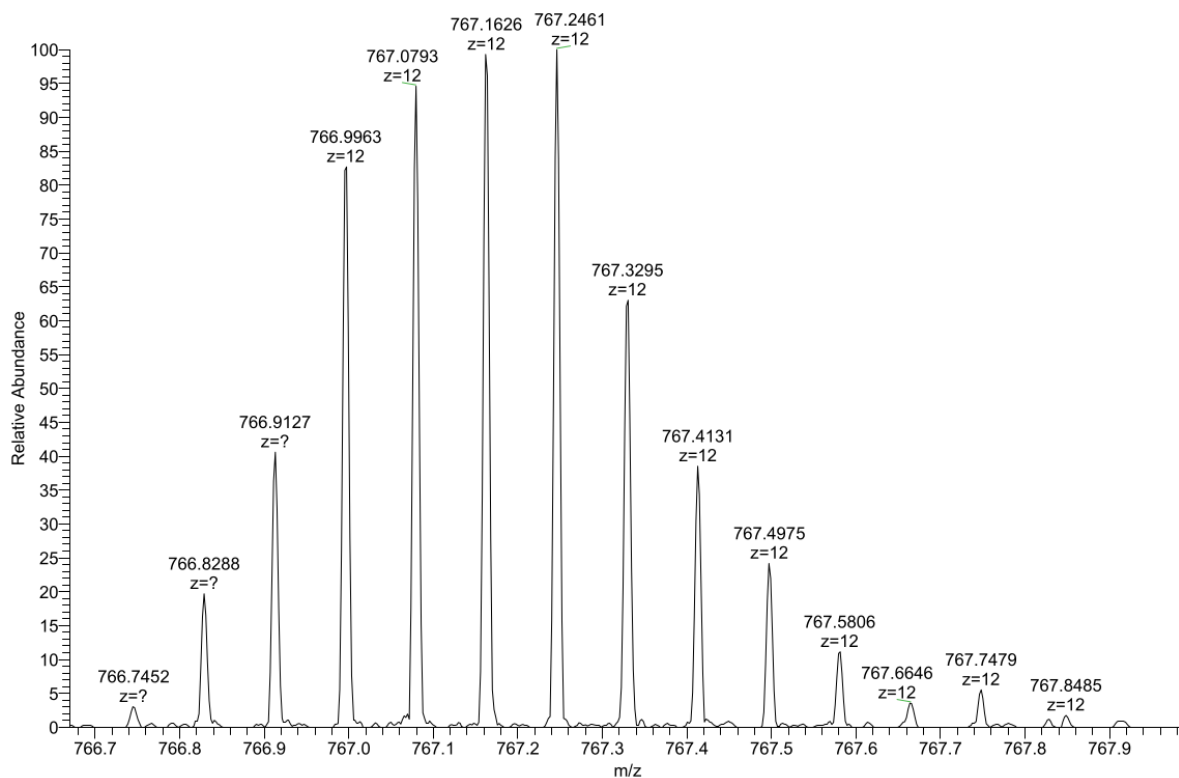
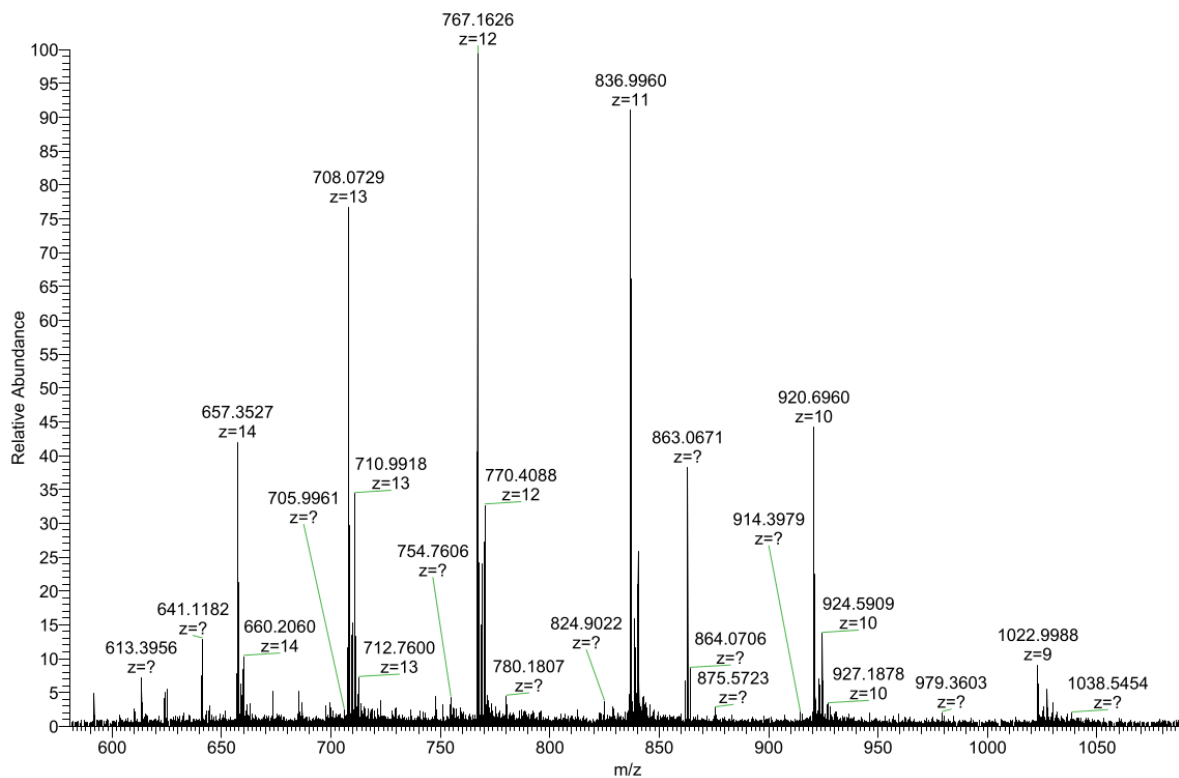


Fig. S3 MS spectra of ON2.



**Fig. S4** MS spectra of ON3.

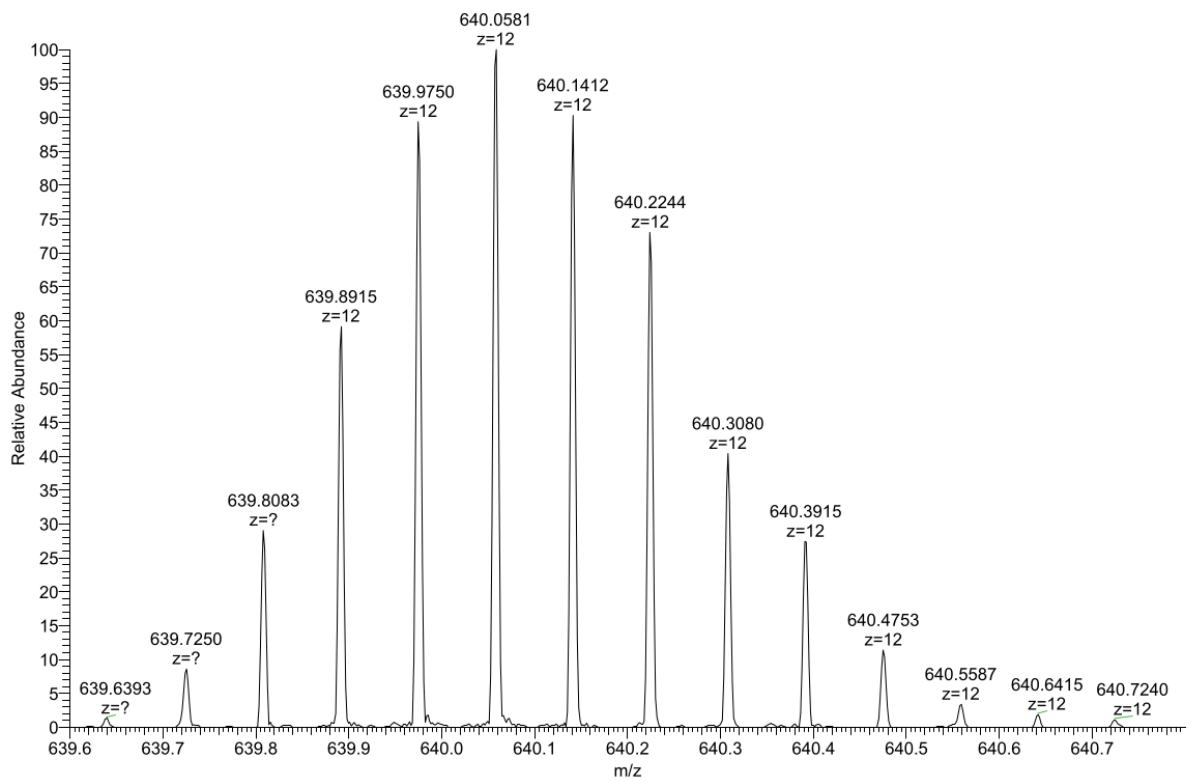
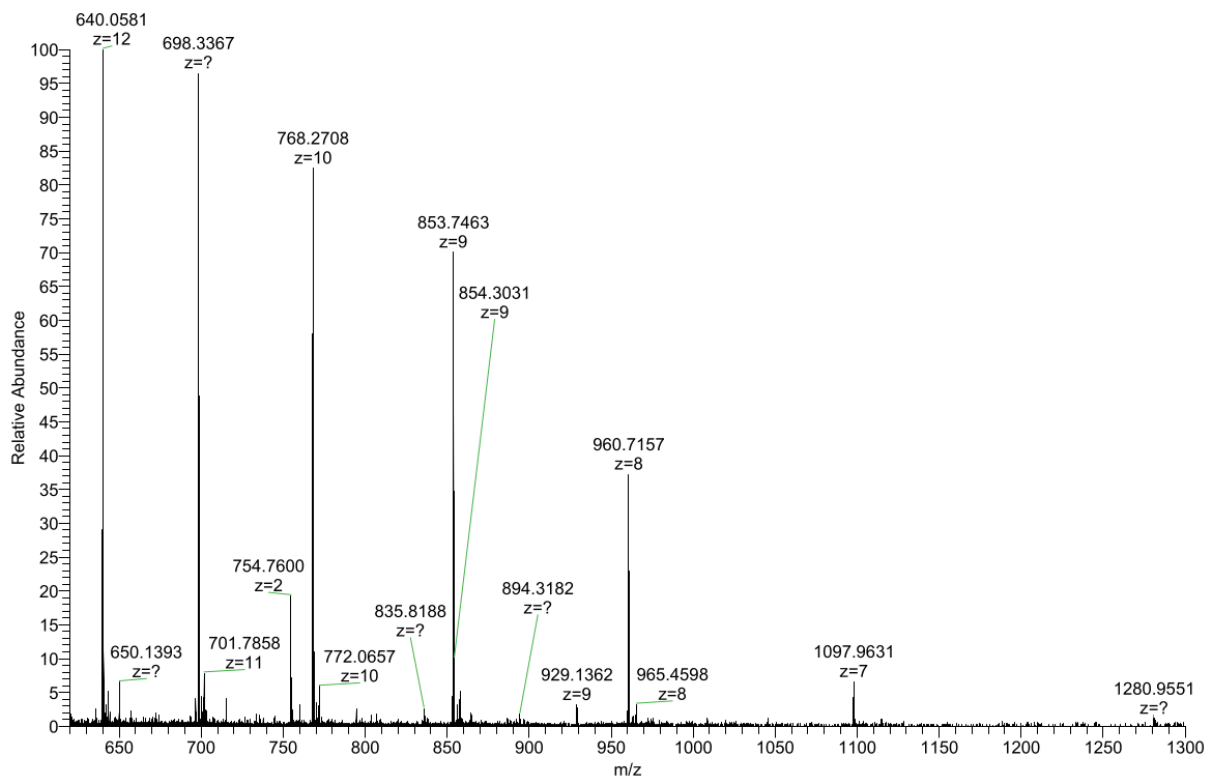


Fig. S5 MS spectra of ON4.



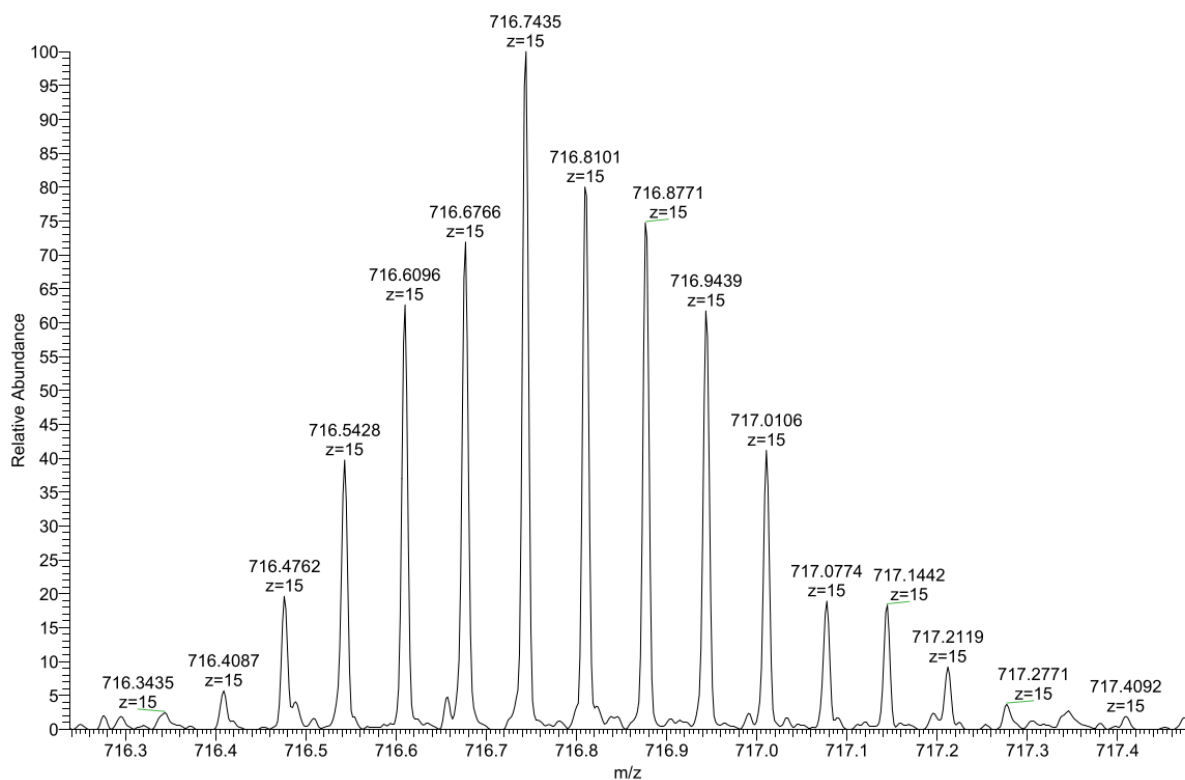
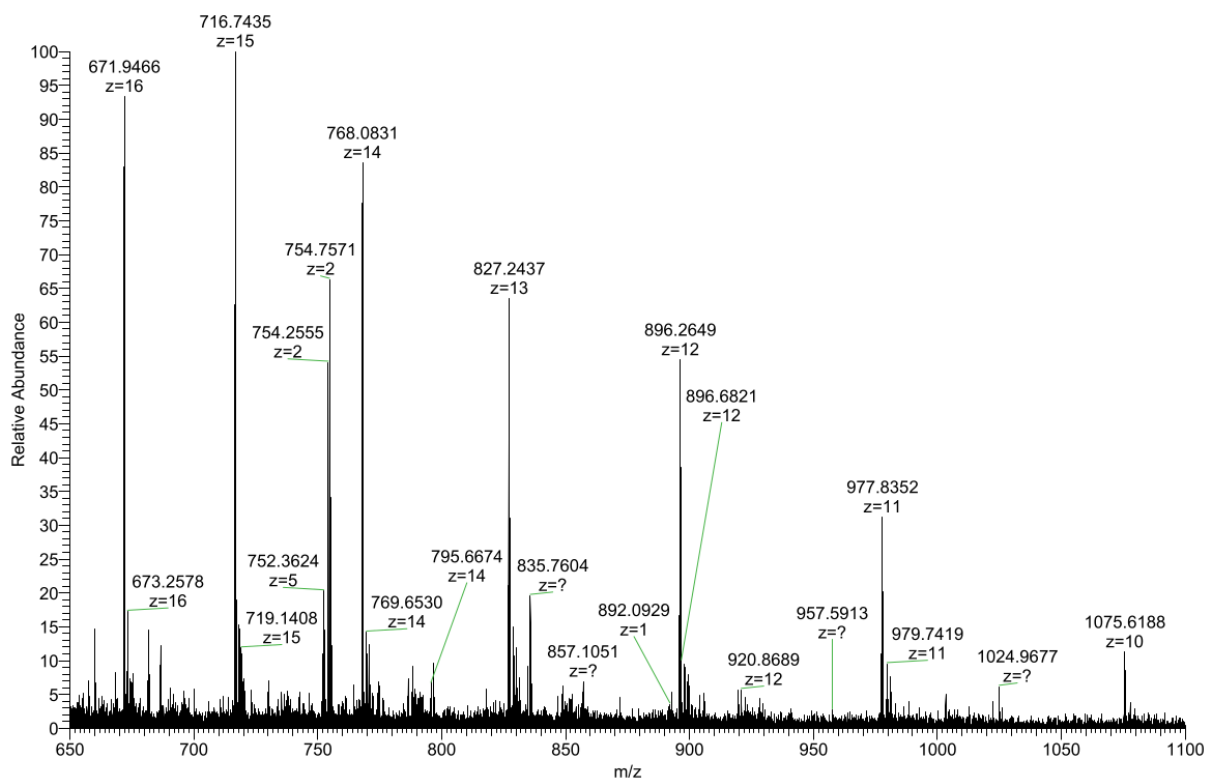
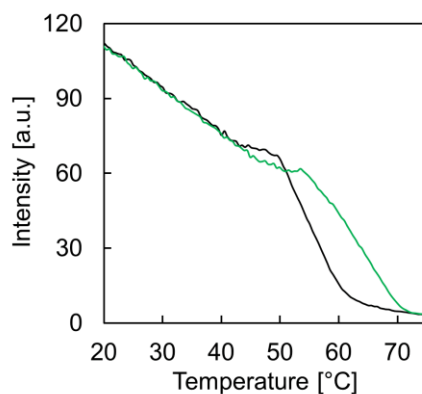
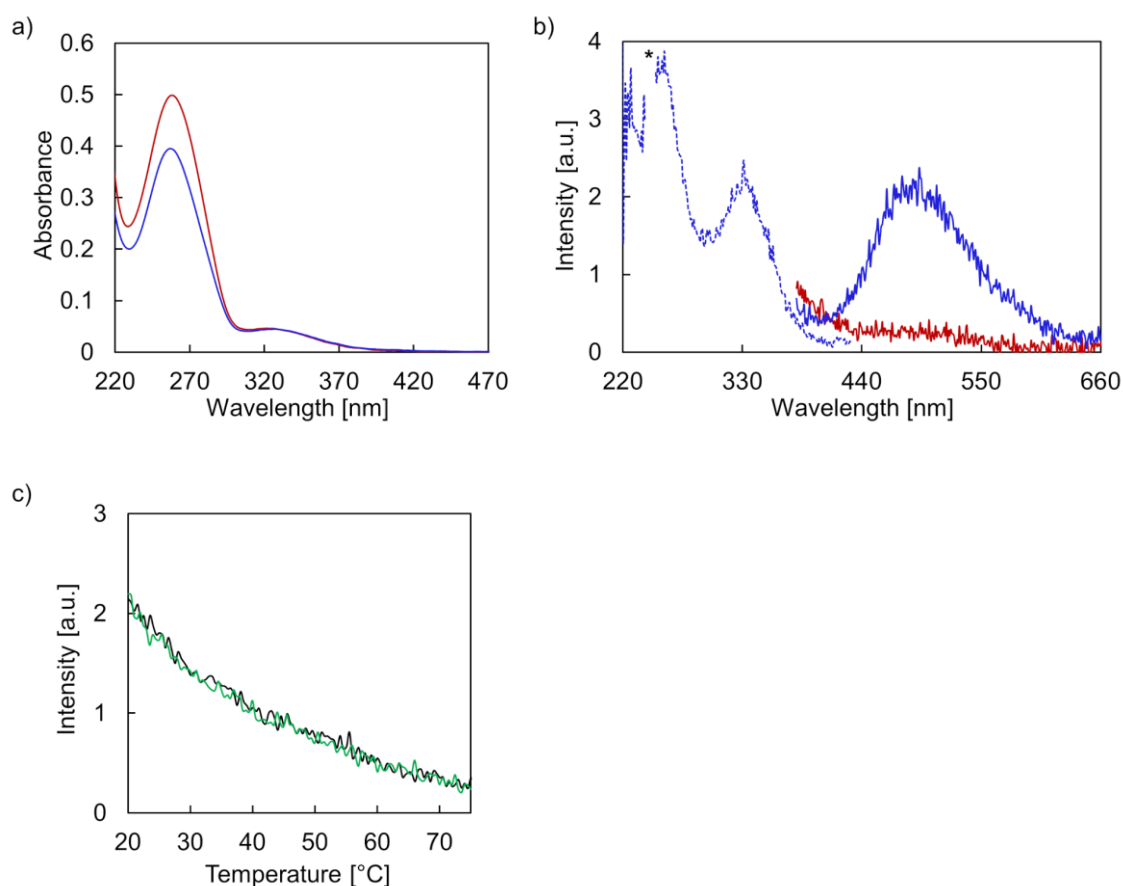


Fig. S6 MS spectra of ON5.

### 3. UV-Vis and fluorescence spectra



**Fig. S7** Fluorescence-monitored annealing (black) and melting (green) curves of **3**. Conditions: 1  $\mu\text{M}$  **3**, 10 mM sodium phosphate buffer pH 7.2, 0.1 mM spermine  $\cdot$  4 HCl, 20 vol% ethanol, 0.5  $^{\circ}\text{C}/\text{min}$ ,  $\lambda_{\text{ex}}$ : 335 nm,  $\lambda_{\text{em}}$ : 490 nm.



**Fig. S8** Temperature-dependent UV-Vis absorption spectra of **1** (a), temperature-dependent fluorescence emission (b, solid line) and excitation (b, dotted line) spectra of **1** at 75  $^{\circ}\text{C}$  (red) and at 20  $^{\circ}\text{C}$  (blue) after thermal assembly process (0.5  $^{\circ}\text{C}/\text{min}$ ; \* denotes second-order diffraction). (c) Fluorescence-monitored annealing (black) and melting (green) curves of **1**. Conditions: 1  $\mu\text{M}$  **1**, 10 mM sodium phosphate buffer pH 7.2, 0.1 mM spermine  $\cdot$  4 HCl, 20 vol% ethanol,  $\lambda_{\text{ex}}$ : 335 nm,  $\lambda_{\text{em}}$ : 490 nm.

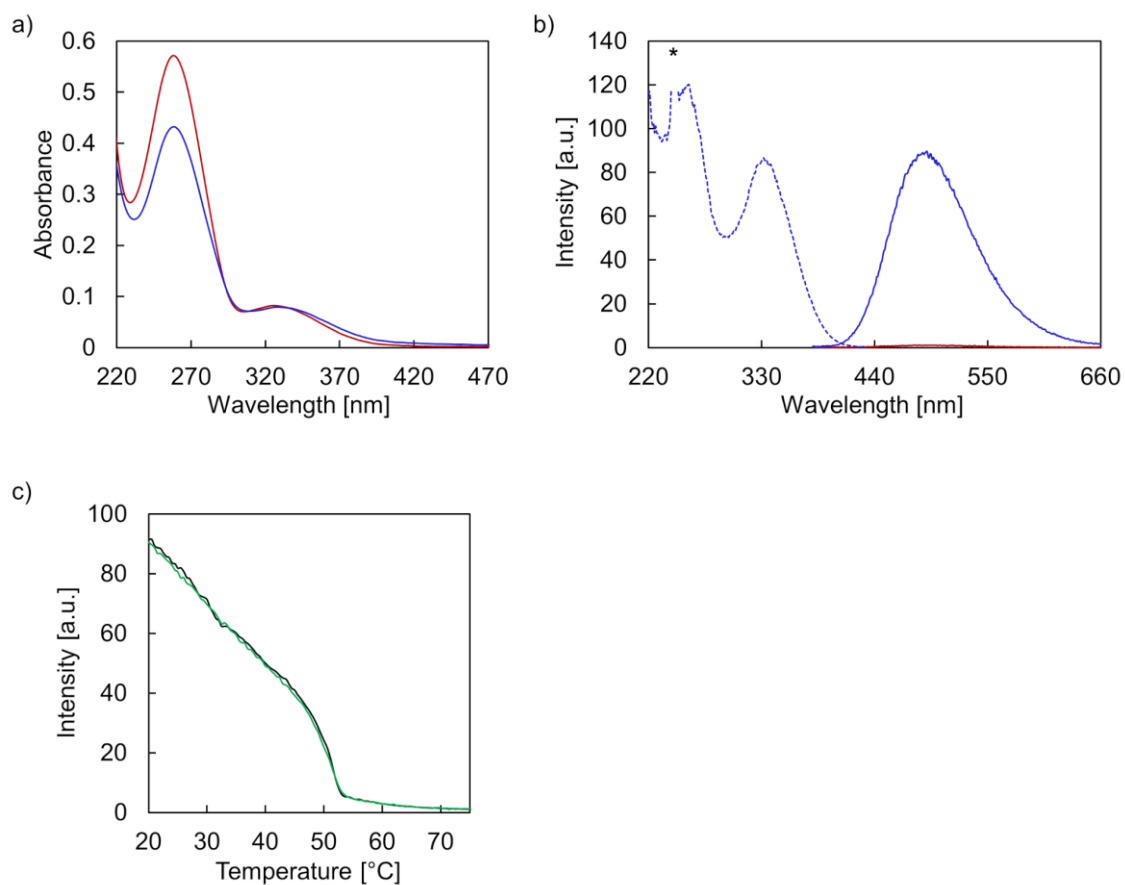


**Fig. S9** Temperature-dependent UV-Vis absorption spectra of **2** (a), temperature-dependent fluorescence emission (b, solid line) and excitation (b, dotted line) spectra of **2** at 75 °C (red) and at 20 °C (blue) after thermal assembly process (0.5 °C/min; \* denotes second-order diffraction). (c) Fluorescence-monitored annealing (black) and melting (green) curves of **2**. Conditions: 1  $\mu$ M **2**, 10 mM sodium phosphate buffer pH 7.2, 0.1 mM spermine  $\cdot$  4 HCl, 20 vol% ethanol,  $\lambda_{\text{ex.}}$ : 335 nm,  $\lambda_{\text{em.}}$ : 490 nm.

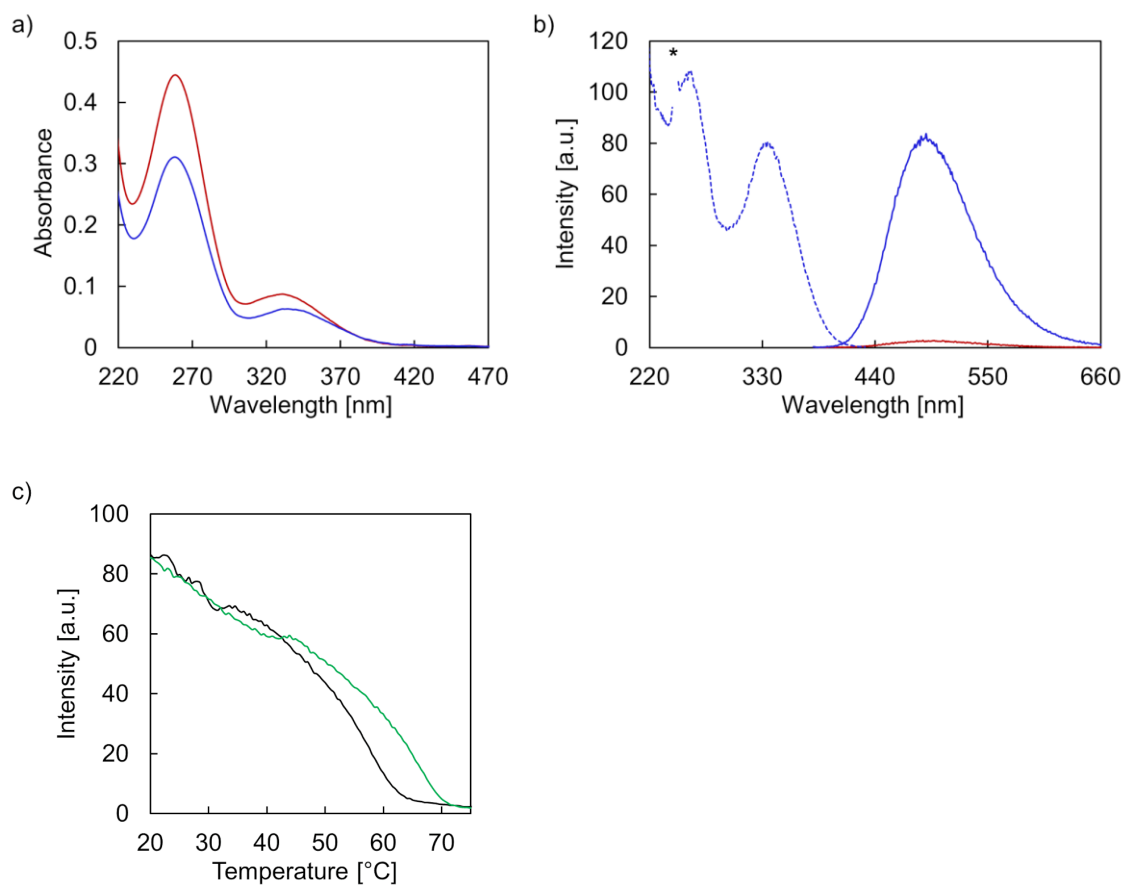


**Fig. S10** Temperature-dependent UV-Vis absorption spectra of **4** (a), temperature-dependent fluorescence emission (b, solid line) and excitation (b, dotted line) spectra of **4** at 75 °C (red) and at 20 °C (blue) after thermal assembly process (0.5 °C/min; \* denotes second-order diffraction). (c) Fluorescence-monitored annealing (black) and melting (green) curves of **4**. Conditions: 1  $\mu$ M **4**, 10 mM sodium phosphate buffer pH 7.2, 0.1 mM spermine  $\cdot$  4 HCl, 20 vol% ethanol,  $\lambda_{\text{ex}}$ : 335 nm,  $\lambda_{\text{em}}$ : 490 nm.

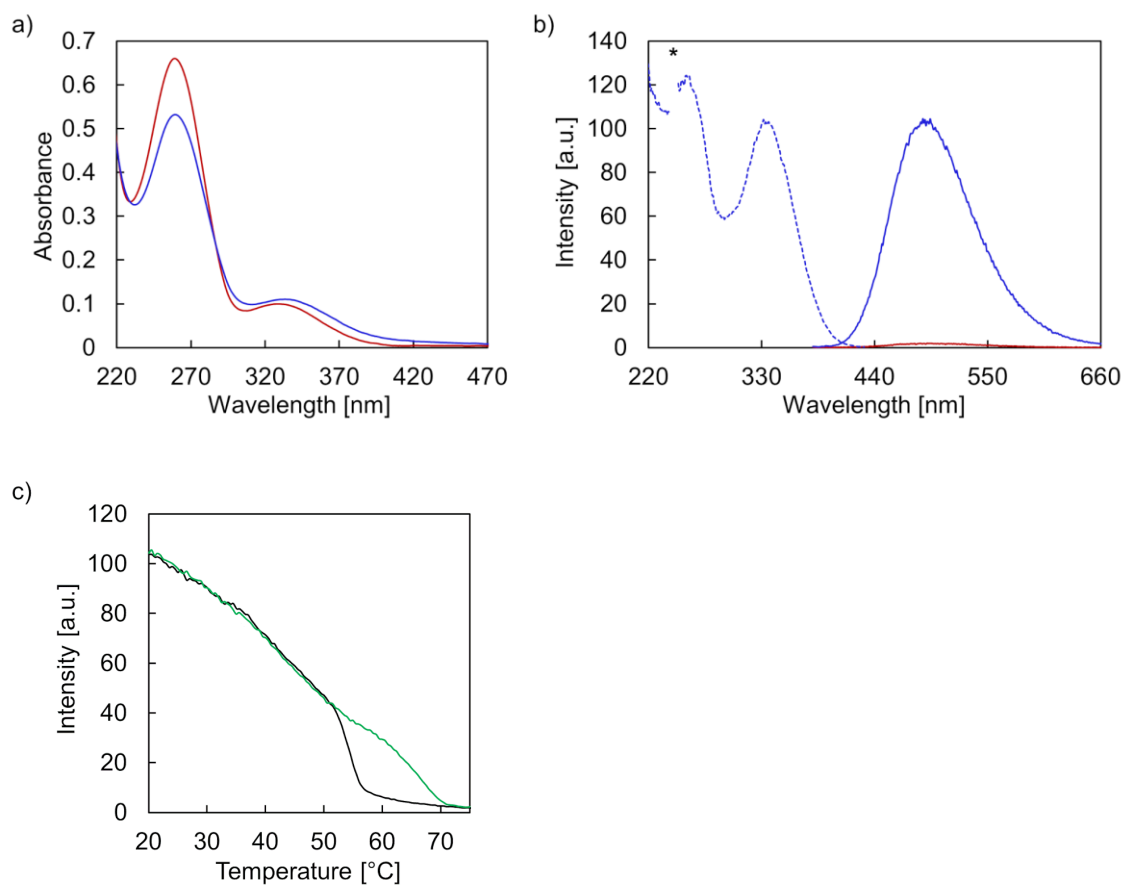


**Fig. S11** Temperature-dependent UV-Vis absorption spectra of **5** (a), temperature-dependent fluorescence emission (b, solid line) and excitation (b, dotted line) spectra of **5** at 75 °C (red) and at 20 °C (blue) after thermal assembly process (0.5 °C/min; \* denotes second-order diffraction). (c) Fluorescence-monitored annealing (black) and melting (green) curves of **5**. Conditions: 1  $\mu$ M **5**, 10 mM sodium phosphate buffer pH 7.2, 0.1 mM spermine  $\cdot$  4 HCl, 20 vol% ethanol,  $\lambda_{\text{ex}}$ : 335 nm,  $\lambda_{\text{em}}$ : 490 nm.

#### 4. AFM images

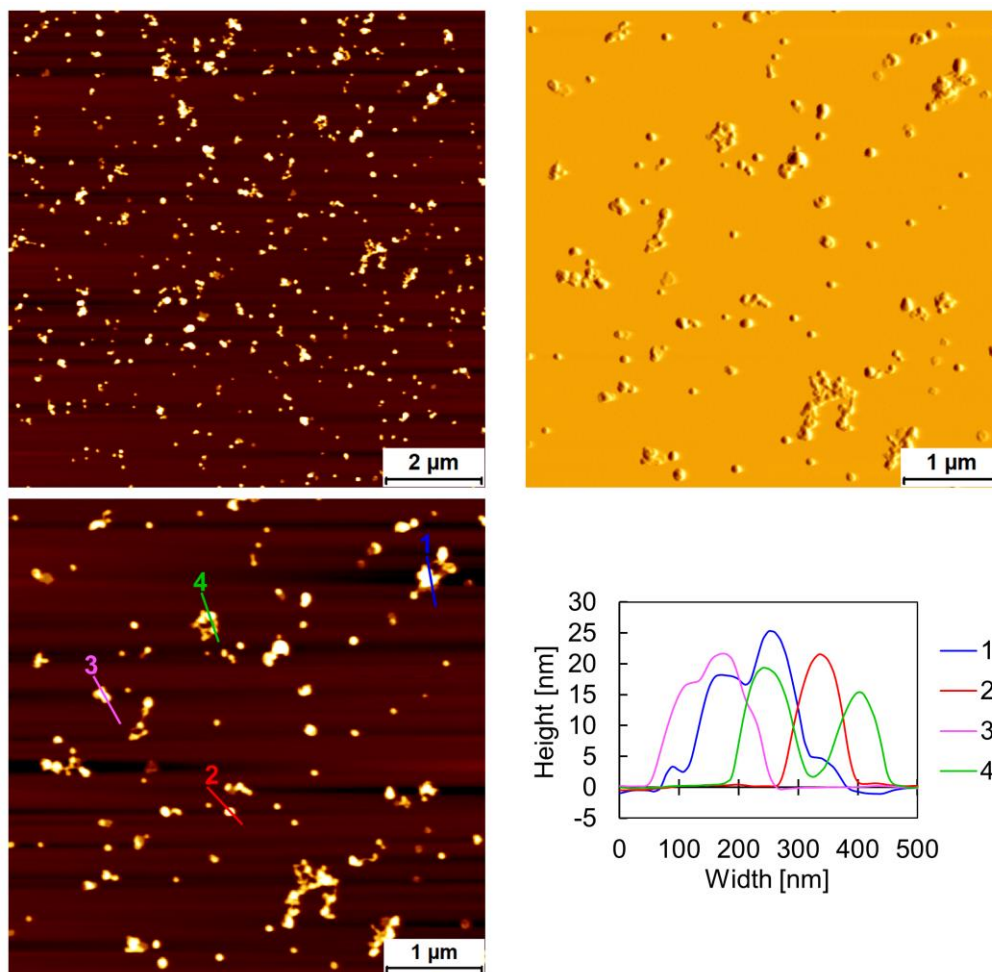


**Fig. S12** AFM overview scan (top left), deflection scan (top right), and zoom with corresponding cross sections (bottom) of assembled duplex **3**. Conditions: 1 μM **3**, 10 mM sodium phosphate buffer pH 7.2, 0.1 mM spermine · 4 HCl, 20 vol% ethanol.

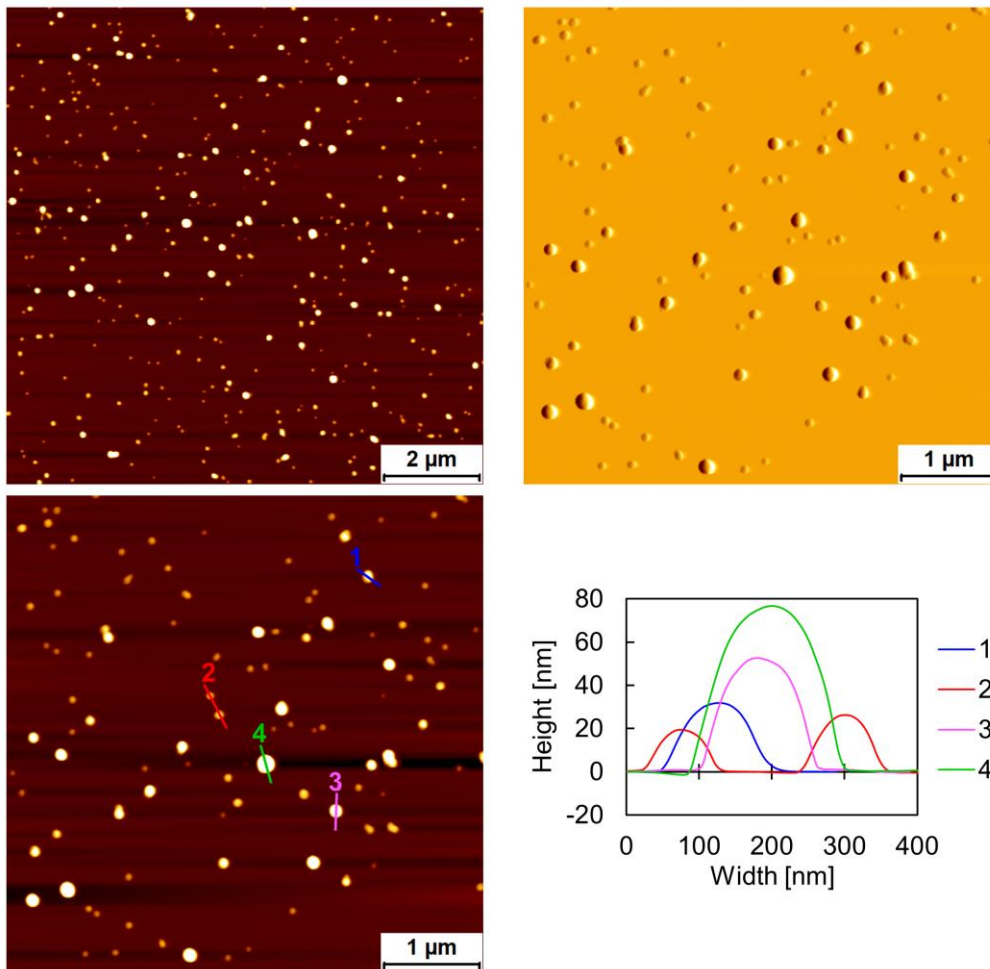


**Fig. S13** AFM overview scan (top left), deflection scan (top right), and zoom with corresponding cross sections (bottom) of assembled duplex **2**. Conditions: 1 μM **2**, 10 mM sodium phosphate buffer pH 7.2, 0.1 mM spermine · 4 HCl, 20 vol% ethanol.

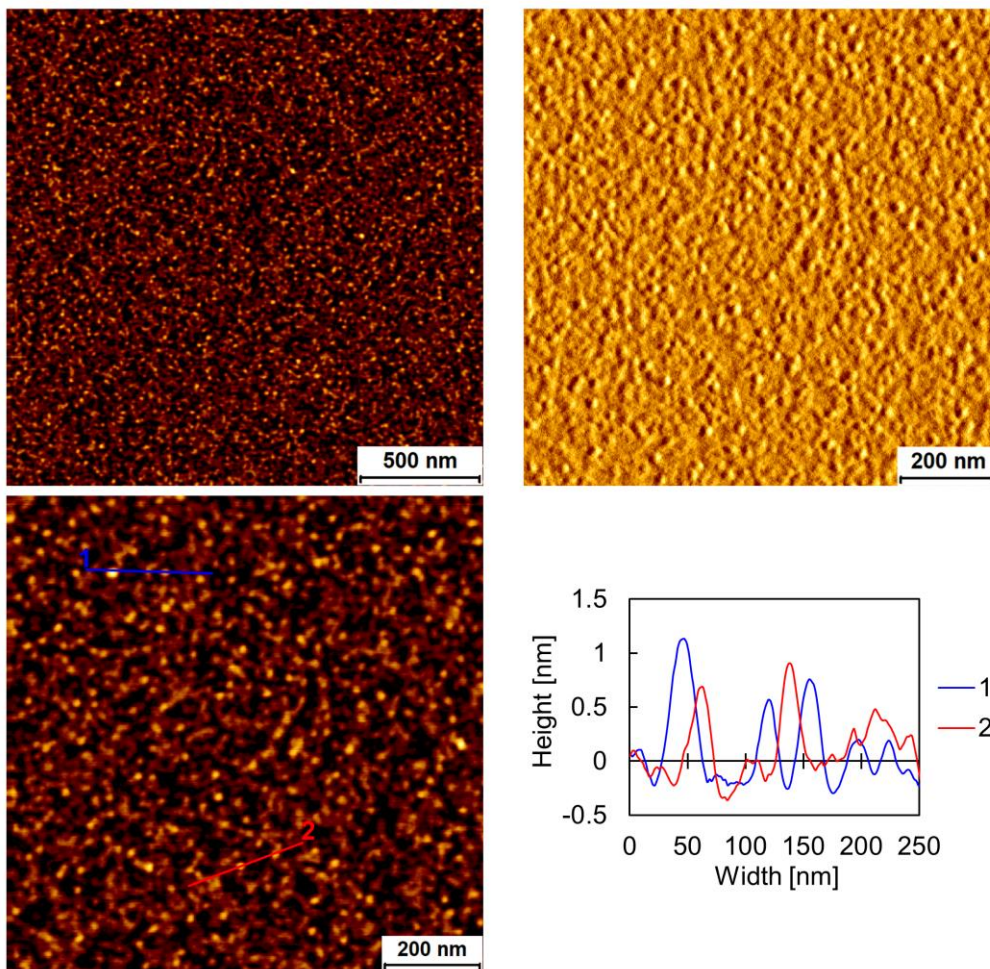


**Fig. S14** AFM overview scan (top left), deflection scan (top right), and zoom with corresponding cross sections (bottom) of assembled duplex **1**. Conditions: 1  $\mu\text{M}$  **1**, 10 mM sodium phosphate buffer pH 7.2, 0.1 mM spermine  $\cdot$  4 HCl, 20 vol% ethanol.



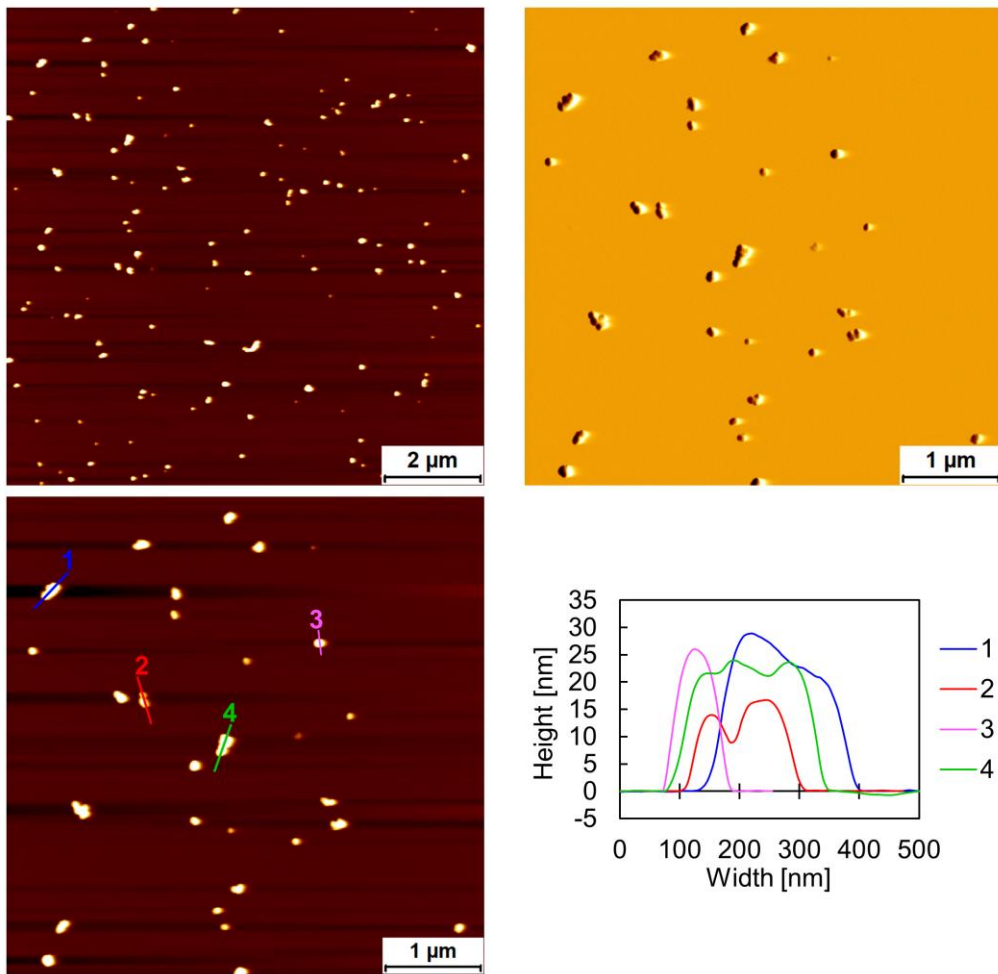


**Fig. S15** AFM overview scan (top left), deflection scan (top right), and zoom with corresponding cross sections (bottom) of assembled duplex **4**. Conditions: 1 μM **4**, 10 mM sodium phosphate buffer pH 7.2, 0.1 mM spermine · 4 HCl, 20 vol% ethanol.

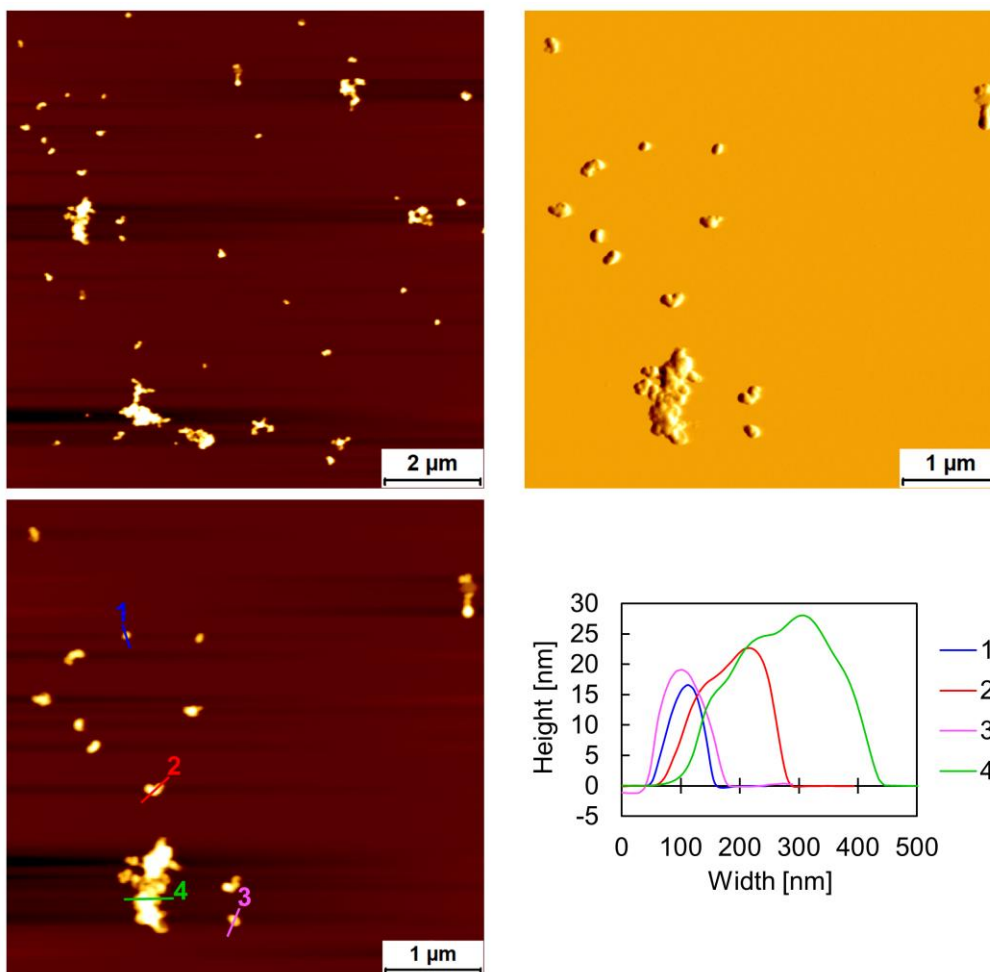


**Fig. S16** AFM overview scan (top left), deflection scan (top right), and zoom with corresponding cross sections (bottom) of assembled duplex **5**. Conditions: 1 μM **5**, 10 mM sodium phosphate buffer pH 7.2, 0.1 mM spermine · 4 HCl, 20 vol% ethanol.

## 5. DLS

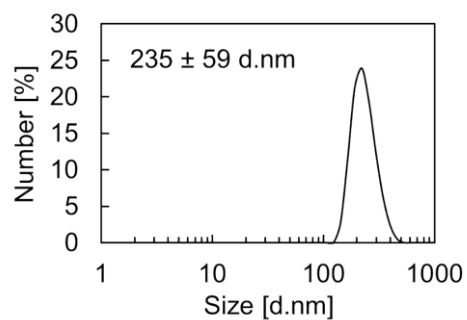


**Fig. S17** DLS of vesicles assembled from duplex **2**. Conditions: 1  $\mu\text{M}$  **2**, 10 mM sodium phosphate buffer pH 7.2, 0.1 mM spermine  $\cdot$  4 HCl, 20 vol% ethanol.

## 6. Cryo-EM images

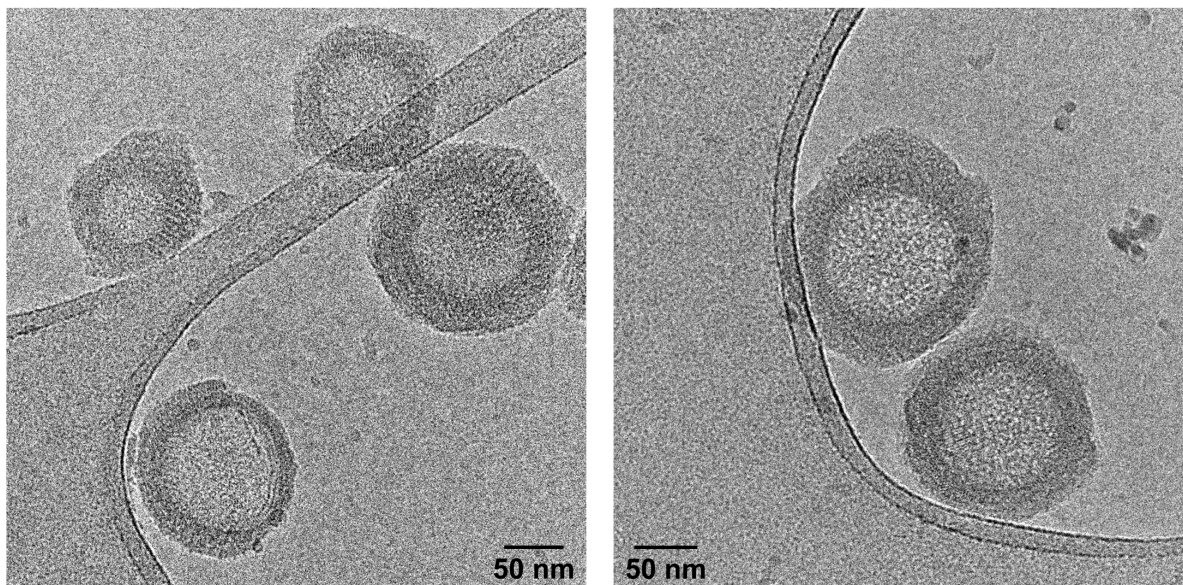


**Fig. S18** Additional cryo-EM images of assembled duplex **3**. Conditions: 1  $\mu\text{M}$  **3**, 10 mM sodium phosphate buffer pH 7.2, 0.1 mM spermine  $\cdot$  4 HCl, 30 vol% ethanol.

## 7. Bibliography

- 1 S. Rothenbühler, I. Iacovache, S. M. Langenegger, B. Zuber and R. Häner, *Nanoscale*, 2020, **12**, 21118–21123.
- 2 J. Schindelin, I. Arganda-Carreras, E. Frise, V. Kaynig, M. Longair, T. Pietzsch, S. Preibisch, C. Rueden, S. Saalfeld, B. Schmid, J.-Y. Tinevez, D. J. White, V. Hartenstein, K. Eliceiri, P. Tomancak and A. Cardona, *Nat. Methods*, 2012, **9**, 676–682.
- 3 M. Linkert, C. T. Rueden, C. Allan, J.-M. Burel, W. Moore, A. Patterson, B. Loranger, J. Moore, C. Neves, D. MacDonald, A. Tarkowska, C. Sticco, E. Hill, M. Rossner, K. W. Eliceiri and J. R. Swedlow, *J. Cell Biol.*, 2010, **189**, 777–782.